SEMARAK ILMU PUBLISHING

Journal of Advanced Research in Fluid Mechanics and Thermal Sciences

Journal homepage:
https://semarakilmu.com.my/journals/index.php/fluid_mechanics_thermal_sciences/index
ISSN: 2289-7879

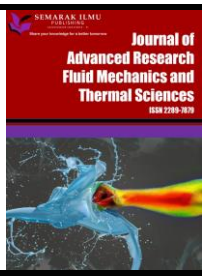

Prediction of Fluid Pattern of Biodiesel Production in a Membrane Reactor

Muhammad Asyraaf Asri[1], Nurul Fitriah Nasir[1,*], Ishkrizat Taib[2], Djamal Hissein Didane[3]

[1] Energy Technology Research Group, Faculty of Mechanical and Manufacturing Engineering, Universiti Tun Hussein Onn Malaysia (UTHM), 86400 Parit Raja, Batu Pahat, Johor, Malaysia
[2] Flow Analysis, Simulation, and Turbulence Research Group, Faculty of Mechanical and Manufacturing Engineering, Universiti Tun Hussein Onn Malaysia (UTHM), 86400 Parit Raja, Batu Pahat, Johor, Malaysia
[3] Centre for Energy and Industrial Environment Studies (CEIES), Faculty of Mechanical and Manufacturing Engineering, Universiti Tun Hussein Onn Malaysia (UTHM), 86400 Parit Raja, Batu Pahat, Johor, Malaysia

ARTICLE INFO

Article history:
Received 10 July 2023
Received in revised form 20 October 2023
Accepted 2 November 2023
Available online 15 November 2023

Keywords:
Biodiesel; membrane reactor; Computational Fluid Dynamic; renewable energy; separation; fluid pattern

ABSTRACT

Utilization of membrane reactors for biodiesel production has been an alternative to conventional batch reactors. The membrane in the reactor acts as a separation layer, preventing the formation of by-products and allowing the desired biodiesel product to pass through. This can improve yields and reduce waste, making the process more environmentally friendly and economically viable. This study aimed to analyze the fluid flow and velocity profile inside the membrane reactor and determine the volume fraction of biodiesel. The modeling and simulation of the fluid flow of biodiesel in a membrane reactor was carried out using SOLIDWORK and ANSYS software. Using a Eulerian-Eulerian two-fluid model, multiphase simulations were carried out. Three different temperatures, 333 K, 338 K, and 343 K, were used in the simulation. The results have found that at 333K, the biodiesel production in the membrane reactor shows the best flow characteristics compared to reaction temperatures of 338 K and 343 K. Additionally, the highest volume fraction can be predicted at the temperature of 333K. Further research and simulation study can be implemented to explore the effects of inlet velocity and reaction time on the fluid flow pattern of biodiesel inside the membrane reactor.

1. Introduction

Biodiesel can be made from a variety of feedstocks using a variety of processes. Transesterification, direct mixing, micro-emulsion, and pyrolysis are some of the processes used [1-3]. Furthermore, biodiesel feedstocks include virgin oil (such as rapeseed oil or palm oil), animal fats, used oil (such as yellow grease), and micro- algal oils [4,5]. It provides many benefits to the environment such as reducing carbon dioxide emission, greenhouse gases, and acid rain forming sulfur dioxide. Fossil fuels are the slowest-growing source of energy, and stocks are dwindling every day. Increasing demand for energy will raise prices over the projection period. The combustion of

* *Corresponding author.*
E-mail address: fitriah@uthm.edu.my

https://doi.org/10.37934/arfmts.111.1.156165

fossil fuels emits carbon dioxide, sulfur dioxide, hydrocarbons, and volatile organic compounds (VOCs), which can cause air pollution, global warming, and climate change [6,7]. These negative environmental repercussions are the focus of current energy policies that emphasize cleaner, more efficient, and environmentally friendly technology to boost energy supply and usage [8]. Thus, alternative renewable energy sources are vital for environmental and economic growth. Biodiesel is abundantly available from inexhaustible feedstocks that can lower production costs. Through the chemical reaction's transesterification and esterification, biodiesel is produced [9-11]. Transesterification is the process by which triglycerides (TG), the primary component of vegetable oils and animal fats, are combined with short-chain alcohols, primarily methanol (MeOH), to produce fatty acid methyl esters (FAME), often known as biodiesel [12]. Recent research has shown the utilization of membrane reactors as an alternative to the conventional reactor [13-17]. This research aimed to investigate the fluid flow and velocity profile inside the membrane reactor (MR) using ANSYS Fluent version 22. The flow characteristics and flow pattern were analysed at different reaction temperatures (333K, 338K, and 343K).

2. Methodology

2.1 Geometry of Membrane and Software Selection

In this research, ANSYS FLUENT 2022 R1 was used for all computational fluid dynamics simulations. For the geometric modelling, SOLID WORKS 2020 is used to create the design. Then, the model is imported into ANSYS Workbench for additional analysis. Figure 1 is a sketch of the MR model and Figure 2 is a sketch inside the model. Table 1 lists the dimensions of and physical condition of MR.

Table 1
MR Used in Simulation: Geometry and Physical Conditions

Parameter	Definition
Size of Membrane Reactor	L x d = 421 mm x 40 mm
Size of inlet Pipe	L x d =400 mm x 6 mm
Size of outlet Pipe	L x d = 400 mm x 6 mm
Mass Flow Rate	4g/min
Phase	Fluid

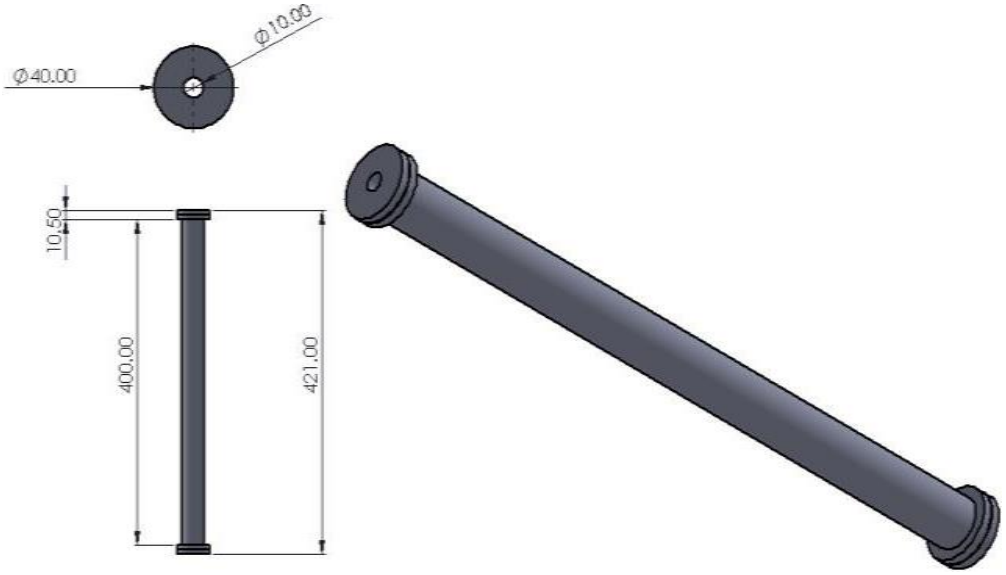

Fig. 1. MR modelling in SOLIDWORK

Fig. 2. Inside drawing of the membrane reactor

Based on Figure 1 and Figure 2, the model consists of two primary components which are the housing and the body of the reactor. At the housing of the reactor, there are an entrance and exit of flow, while there are 7 hollow cylinders with 6 mm diameter inside the reactor.

2.2 Pre-Processor and Meshing

The pre-processor stage utilized SOLID WORKS 2020 for design and the Meshing Design Modeler included in the ANSYS FLUENT packages. The accuracy of CFD is affected by the number of cells in the mesh. In general, a larger number of cells will result in more precise solutions. The geometry was meshed using three different grid sizes: coarse, medium, and fine, as illustrated in Figure 3 to ensure that the solution was grid-size independent.

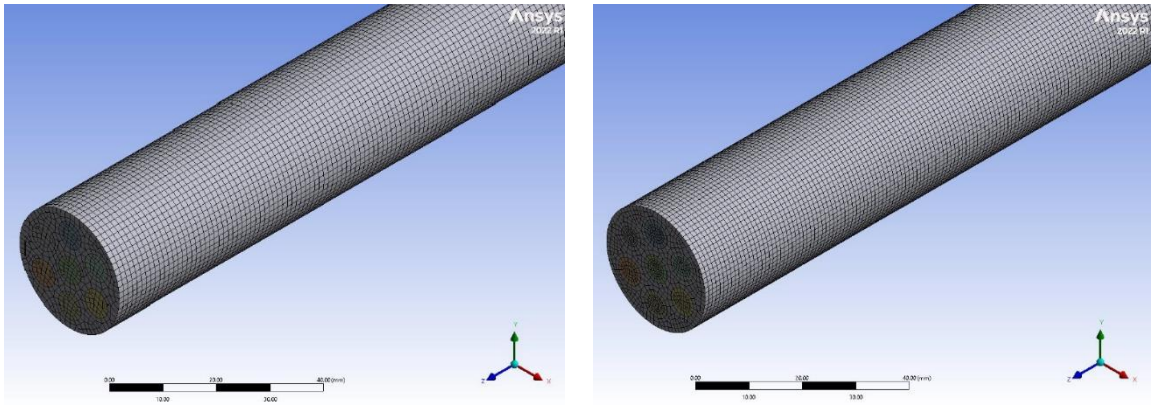

(a) (b)

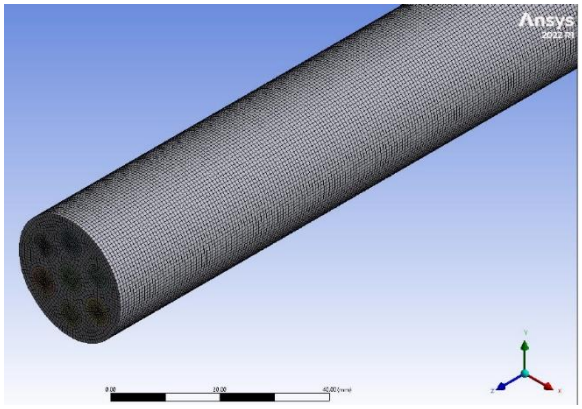

(c)

Fig. 3. Type of meshing in the membrane reactor (a) Coarse (b) Medium (c) Fine

Table 2 shows the grid independence test results. Reducing the element size is good, but since the results are similar to the medium set up, therefore medium meshing was selected. Thus, it reduces the calculation time for each run. Element 1.0 was selected for this study.

Table 2
Grid Independence Test for Membrane Reactor

Element	Number of nodes	Number of elements	Skewness mesh matric	Orthogonal mesh matric	Element quality
1.2	413784	347918	0.78117	0.22009	0.99635
1.1	411941	345591	0.67626	0.37501	0.99487
1.0	451457	381492	0.55803	0.57687	0.99823
0.9	584285	502608	0.57914	0.42086	0.99972
0.8	801099	696500	0.71461	0.28539	0.99873
0.7	1244100	1114021	0.5344	0.4656	0.99943

2.3 Boundary Conditions, Solver Setup and Computational Model

At the intake, the velocity is set at 2 m/s. At the inlets and outlets, turbulent kinetic energy and dissipation rate are set to O since it is difficult to evaluate the effects of turbulence at the boundaries. The Euler – Euler model treats both phases as continuous phases, meaning that the gas phase does not move along the wall, therefore, no-slip boundary condition is applied to the gas phase along the wall. Table 3 summarizes the boundary condition for the MR and Table 4 provides information for the solver setup in CFD simulation. The computational model was referred to previous studies and analysis [18,19].

Table 3
Summary of Boundary Conditions in MR Simulation

Boundary Condition	Parameter
Domain/interior	FAME
Wall	Reactor (no-slip)
Velocity Inlet	2 m/s
Inlet pressure gauge	0.1 Mpa

Table 4
Setting for solver setup in FLUENT

Option	Type
Model	3D
Gravitational acceleration	9.81 m/s^2
Multiphase model	Volume of fluid (VOF)
Viscous model	Standard k-e Standard wall F
Material	Methyl-alcohol-vapor(ch3oh) triglyceride
Phases	Vapor (Methyl-alcohol-vapor) Oil (triglyceride)
Operating pressure	101.325 Pa
Operating density	844.8 kg/m^3
Surface tension (oil-vapor)	0.0586 (N/m)

3. Results

3.1 Flow Pattern

The flow patterns in the reactor were predicted at each temperature. Two thousand iterations were used in the calculation setup, with time steps of 0.001s. Using the XY Plane as the viewing angle, the results show how glycerol and biodiesel were mixed and how the fluid flows into the reactor. Figure 4 shows the contours of the volume fraction at 333 K, 338K, and 343K, which explains how glycerol is distributed throughout the biodiesel oil. Red contours denote the volume fraction of 1 and the blue color shows that the volume fraction is 0. The flow pattern of the membrane reactor illustrated how 5 K temperature setups would produce different fluid patterns. The volume fraction begins with 0 at each temperature setting, however, at 333K, the combination of biodiesel and glycerol begins to rise at a rate of 6.147e^{-02} from the reactor input to its output. In addition, 333 K and 338 K achieve highest volume fraction which is 9.655 e-01 meaning that it produces a good quality of biodiesel plus the red contour show that the 333 K produce more biodiesel than other temperature. The flow regime flow has heterogeneous flow for all temperature settings. Establishing an annular flow regime is visible at all three flow temperatures. In essence, annular flow is stable and appears as velocity increases.

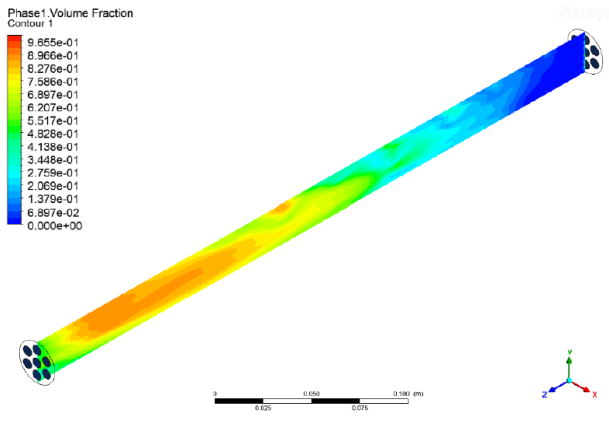

(a)

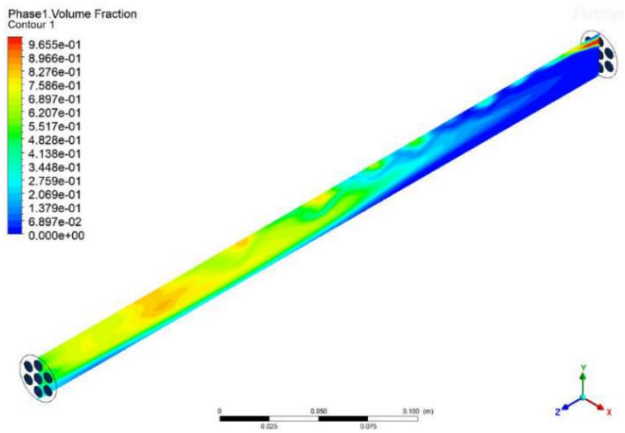

(b)

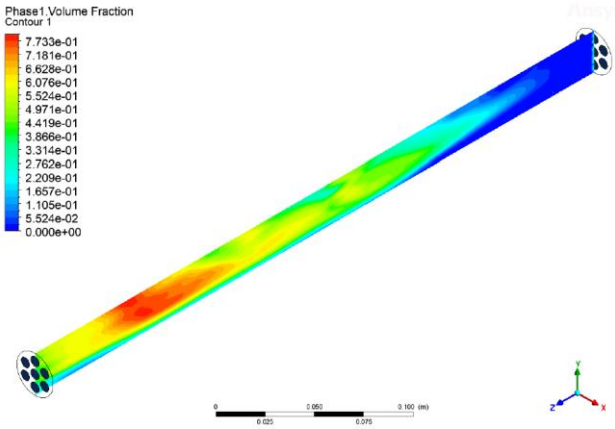

(c)

Fig. 4. Flow pattern of biodiesel (a) at 333 K (b) at 338 K (c) at 343 K

3.2 Streamline

The curves in streamline charts are always tangent to the instantaneous vector field. Additionally, it can be defined as the motion of a fictitious particle suspended in a fluid and the geometric representation of the flow velocity in any scenario in which the fluid is moving. At first, the flow profile is completely formed and turbulent; after that, it transforms into a laminar flow until it reaches the outlet. The streamline of velocity at three distinct temperatures, 333 K, 338 K, and 343 K, was determined from the outcome as shown as Figure 5 below. At 333 K and 338, the streamline direction and pattern are nearly the same, but the range of eddies becomes larger near the wall. The streamline starts to expand and rise across the membrane reactor body to the outlet. Turbulence causes the backflow which raises the contact time between glycerol and biodiesel, thus from the mixture of glycerol and biodiesel.

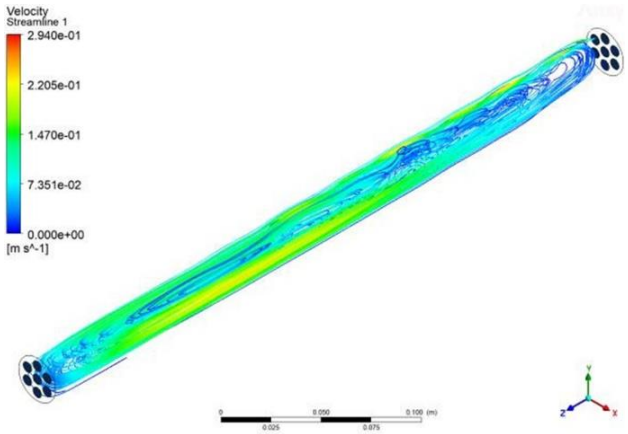

(a)

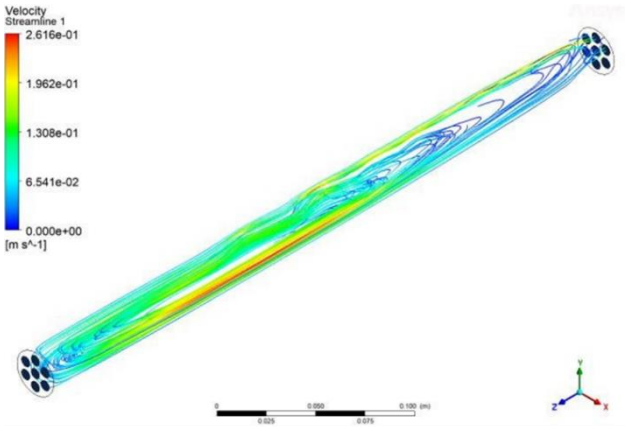

(b)

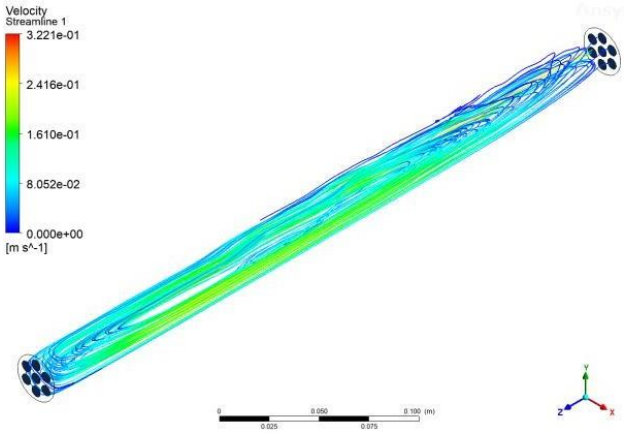

(c)

Fig. 5. Streamline inside membrane reactor (a) at 333 K (b) at 338 K (c) at 343 K

3.3 Velocity Profile of Membrane Reactor for Biodiesel Production

The motion of the flow inside the reactor is referred to as velocity. Turbulence flow occurs when the velocity is high. The velocity dependent on various temperatures is briefly described in this section. Using the XY Plane, the velocity may be determined from the flow inside the reactor. A blue contour indicates the lowest velocity, while the fastest velocity is indicated by red. Figure 6 shows the velocity of biodiesel inside the membrane reactor at different temperatures.

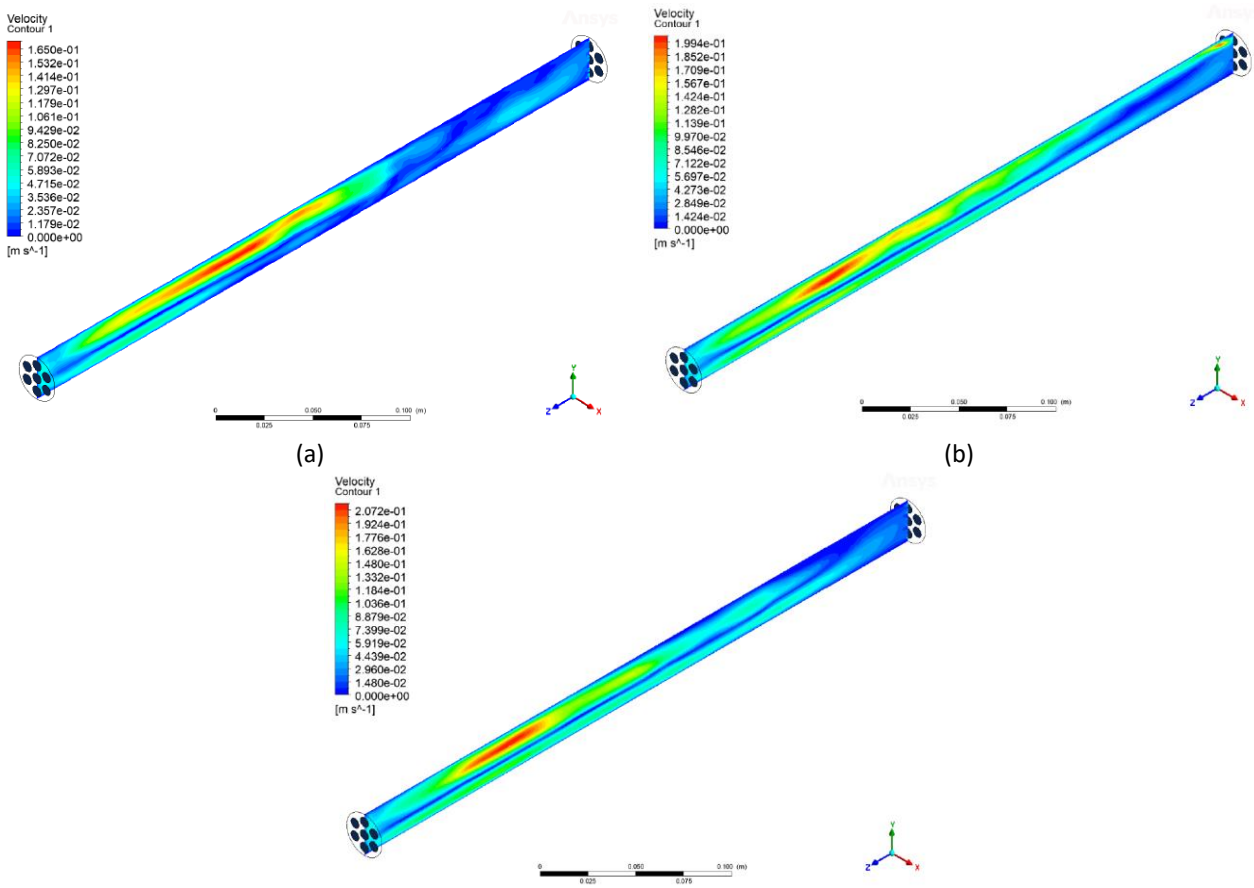

(a) (b)

(c)

Fig. 6. Velocity of biodiesel inside the membrane reactor (a) at 333 K (b) at 338 K (c) at 343 K

At temperature of 333 K, a lower rate of velocity was found, which can reduce the risk of fouling or clogging of the membrane. All components are shown at a steady state, and the production rate slowly decreases. However, the specific characteristics of the velocity profile can vary depending on the design and operating conditions of the reactor. In addition, velocity can affect the residence time of the reaction mixture within the reactor. A longer residence time can provide more opportunity for the reaction to occur, leading to higher conversion rates and improved product quality. However, longer residence times may also increase the risk of product degradation and side reactions.

3.4 Velocity Analysis

The velocity analysis was plotted according to the vertical and horizontal planes, as illustrated in Figure 7. The analysis allows for the selection of the ideal concentration. Additionally, the graph primarily focuses on the velocity result because, during the transesterification process, the velocity can identify whether the flow pattern in the reactor is highly turbulent or in a low-turbulence regime. The plotted velocity against distance at 333K, 338K, and 343K shows the flow characteristics in the membrane reactor along the centerline axis.

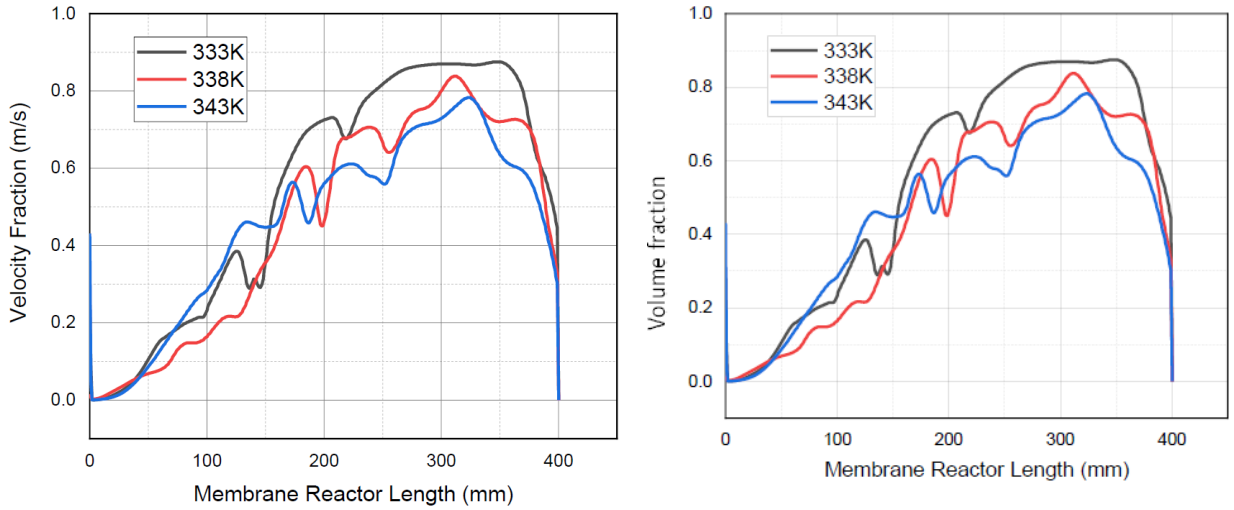

Fig. 7. The flow characteristics in the membrane reactor along the axis of the centerline; (a) Velocity fraction, (b) Volume fraction

Based on Figure 7(a), membrane reactors operating at 333K provide slightly different results than those operating at 343K and 338K. For instance, a steady increase was created at 333K at the start of the flow due to the reaction between glycerol and biodiesel and the low temperature. Furthermore, the fluid velocity largely increases until the middle of the membrane reactor's length. After that point, it starts to decrease and transitions to a steady flow. This might be because biodiesel fuel is reaching the pipe outlet. Figure 7(b) shows the volume fraction along the membrane reactor. Among the other temperatures, 333 K exhibits the largest volume fraction. This is due to a mixture of glycerol and methyl ester reacting as it enters the reactor. The volume portion then dramatically decreases and changes to a constant flow until they reach the pipe outlet. Previous research has reported that at a temperature of 333K, the maximum conversion of biodiesel was obtained, which in line with the results of the prediction carried out in this study [20].

4. Conclusions

This study aimed to investigate the fluid flow and velocity profile of biodiesel in a membrane reactor. The study has investigated the effects of reaction temperature on the fluid pattern and velocity contour inside the membrane reactor. This study has found that at 333K, the biodiesel production in the membrane reactor shows the best flow characteristics compared to reaction temperatures of 338 K and 343 K. Additionally, it can be predicted that at the temperature of 333K, it exhibits the highest volume fraction. Further study may be conducted to examine the effects of inlet velocity and reaction time on the fluid flow pattern of biodiesel inside the membrane reactor.

Acknowledgement

The authors wish to acknowledge the Registrar Office, Universiti Tun Hussein Onn Malaysia for their financial support of this research work.

References

[1] Sarwani, Muhamad Khairul Ilman, Mas Fawzi, Shahrul Azmir Osman, Anwar Syahmi, and Wira Jazair Yahya. "Calculation of Specific Exhaust Emissions of Compression Ignition Engine Fueled by Palm Biodiesel Blend." *Journal of Advanced Research in Applied Sciences and Engineering Technology* 27, no. 1 (2022): 92-96. https://doi.org/10.37934/araset.27.1.9296

[2] Hayder, G., and P. Puniyarasen. "Identification and evaluation of wastes from biodiesel production process." *Journal of Advanced Research in Applied Sciences and Engineering Technology* 3, no. 1 (2016): 21-29.

[3] Isahak, W. N. R. W., Jamaliah Md Jahim, Manal Ismail, Nurul Fitriah Nasir, Muneer M. Ba-Abbad, and Mohd Ambar Yarmo. "Purification of crude glycerol from industrial waste: Experimental and simulation studies." *Journal of Engineering Science and Technology* 11, no. 8 (2016): 1056-1072.

[4] Veza, Ibham, Mohd Farid Muhamad Said, Djati Wibowo Djamari, Mohd Azman Abas, Zulkarnain Abdul Latiff, and Mohd Rozi Mohd Perang. "Future Direction of Microalgae Biodiesel in Indonesia." *Journal of Advanced Research in Applied Sciences and Engineering Technology* 25, no. 1 (2021): 1-6. https://doi.org/10.37934/araset.25.1.16

[5] Kong, Yu Man, Joon Hin Lee, Kiat Moon Lee, and Wah Yen Tey. "Techniques of improving microalgae in biomass clean energy: A short review." *Progress in Energy and Environment* 10 (2019): 6-20.

[6] Dubé, M. A., A. Y. Tremblay, and J. Liu. "Biodiesel production using a membrane reactor." *Bioresource Technology* 98, no. 3 (2007): 639-647. https://doi.org/10.1016/j.biortech.2006.02.019

[7] Mittelbach, Martin, Manfred Wörgetter, Josef Pernkopf, and Hans Junek. "Diesel fuel derived from vegetable oils: preparation and use of rape oil methyl ester." *Energy in Agriculture* 2 (1983): 369-384. https://doi.org/10.1016/0167-5826(83)90031-1

[8] Hammond, G. P., S. Kallu, and M. C. McManus. "Development of biofuels for the UK automotive market." *Applied Energy* 85, no. 6 (2008): 506-515. https://doi.org/10.1016/j.apenergy.2007.09.005

[9] Nurfitri, Irma, Gaanty Pragas Maniam, Noor Hindryawati, Mashitah M. Yusoff, and Shangeetha Ganesan. "Potential of feedstock and catalysts from waste in biodiesel preparation: a review." *Energy Conversion and Management* 74 (2013): 395-402. https://doi.org/10.1016/j.enconman.2013.04.042

[10] Olagunju, Olusegun Ayodeji, Paul Musonge, and Sammy Lewis Kiambi. "Production and Optimization of Biodiesel in a Membrane Reactor, Using a Solid Base Catalyst." *Membranes* 12, no. 7 (2022): 674. https://doi.org/10.3390/membranes12070674

[11] Ding, Jincheng, Shaokang Qu, Enmin Lv, Jie Lu, and Weiming Yi. "Mini review of biodiesel by integrated membrane separation technologies that enhanced esterification/transesterification." *Energy & Fuels* 34, no. 12 (2020): 15614-15633. https://doi.org/10.1021/acs.energyfuels.0c03307

[12] Huynh, Thien An, and Edwin Zondervan. "Dynamic modeling of fouling over multiple biofuel production cycles in a membrane reactor." *Chemical Product and Process Modeling* 17, no. 2 (2021): 153-170. https://doi.org/10.1515/cppm-2020-0093

[13] Soontarapa, Khantong, Rossarin Ampairojanawong, and Thapanut Palakul. "Esterification and transesterification of palm fatty acid distillate in chitosan membrane reactor." *Fuel* 339 (2023): 126918. https://doi.org/10.1016/j.fuel.2022.126918

[14] Athar, Moina, and Sadaf Zaidi. "Biodiesel Production Technologies." *Biodiesel Technology and Applications* (2021): 241-265. https://doi.org/10.1002/9781119724957.ch8

[15] Hanif, Saman, Mabkhoot Alsaiari, Mushtaq Ahmad, Shazia Sultana, Muhammad Zafar, Farid A. Harraz,

Abdulrahman Faraj Alharbi, Abdulaziz AM Abahussain, and Zubair Ahmad. "Membrane reactor based synthesis of biodiesel from Toona ciliata seed oil using barium oxide nano catalyst." *Chemosphere* 308 (2022): 136458. https://doi.org/10.1016/j.chemosphere.2022.136458

[16] Huynh, Thien An, Vincent Reurslag, Maryam Raeisi, Meik B. Franke, and Edwin Zondervan. "Superstructure Optimization of Biodiesel Production from Continuous Stirred Tank and Membrane Reactors." In *Computer Aided Chemical Engineering*, vol. 49, pp. 109-114. Elsevier, 2022. https://doi.org/10.1016/B978-0-323-85159-6.50018-X

[17] Cao, Peigang, André Y. Tremblay, Marc A. Dubé, and Katie Morse. "Effect of membrane pore size on the performance of a membrane reactor for biodiesel production." *Industrial & Engineering Chemistry Research* 46, no. 1 (2007): 52-58. https://doi.org/10.1021/ie060555o

[18] Suhaimi, A. A., and N. F. Nasir. "Study of the fluid flow pattern in a bubble column reactor for biodiesel production." In *IOP Conference Series: Materials Science and Engineering*, vol. 243, no. 1, p. 012035. IOP Publishing, 2017. https://doi.org/10.1088/1757-899X/243/1/012035

[19] Maksom, Mohammad Syahadan, Nurul Fitriah Nasir, Norzelawati Asmuin, Muhammad Faqhrurrazi Abd Rahman, and Riyadhthusollehan Khairulfuaad. "Biodiesel composition effects on density and viscosity of diesel-biodiesel blend: a CFD study." *CFD Letters* 12, no. 4 (2020): 100-109. https://doi.org/10.37934/cfdl.12.4.100109

[20] Luo, Qingliang, Benqiao He, Mengzhu Liang, Aiqun Kong, and Jianxin Li. "Continuous transesterification to produce biodiesel under HTCC/Na_2SiO_3/NWF composite catalytic membrane in flow-through membrane reactor." *Fuel* 197 (2017): 51-57. https://doi.org/10.1016/j.fuel.2016.12.089